RSC Advances

ROYAL SOCIETY OF CHEMISTRY

www.rsc.org/advances

Journal Name

RSCPublishing

ARTICLE

Metallo-supramolecular grid-type architectures for highly and selectively efficient adsorption of dyes in water†

Cite this: DOI: 10.1039/x0xx00000x

Received 00th January 2012,
Accepted 00th January 2012

DOI: 10.1039/x0xx00000x

www.rsc.org/

Xiaoting Qin,[a] Guonan Zhang,[a] YanfeiGao,[a] Houting Liu,[a] Chunfang Du,[a] Zhiliang Liu*[a,b]

There has been extensive interest in the construction of grid-type supramolecular complexes because of their important roles in material science. However, only few of these compounds have been explored for selective adsorption of dyes. Two novel grid-type architectures composed of mixed valence copper ions and polynitrogen heterocyclic ligand have been successfully synthesized. Interestingly, one of the grid-type architectures with modest grid size could efficiently and selectively adsorb dye molecules.

Introduction

Dyes are widely used in many industries and the generated dyeing wastewaters can cause serious environment pollution and pose a severe health threat to human beings. The remove of synthetic organic dyes from effluents before discharge into natural bodies is an extremely important problem and efficient removal of the dyeing wastewater within a short period of time has attracted growing concerns in research. Among the many physical and chemical approaches, adsorption technology has been shown to be an effective way for removing residual organic pollutants in the wastewaters.[1-3] So far, numerous adsorption methods for the removal of dyes from aqueous environment have been developed. The common adsorbents primarily include activated carbons, zeolites, clays, polymeric materials and so on.[4-7] However, compared with dye adsorption, selective adsorption and separation of dyes are more attractive and challenging for researchers.[8-9]As a matter of fact, the coordination polymers as potential selective adsorbents have received much attention[10-11]. However, grid-type architectures, as a kind of coordination compounds, possess void space accessible to guest molecules, providing an important opportunity for developing new adsorption materials, have been little reported.

As an emerging research area, metallo-supramolecular grid-type architectures have attracted great attention as potential candidates for functional molecular materials.[12-13] In particular, grid-type architectures that are composed of mixed-valence metal ions have become an active area of research owning to their functional features such as magnetic[14-15], electrochemical[16] and spectroscopicproperties[17]. Furthermore, grid-type architectures with appropriate pores may provide adequate space to accommodate dye molecules. With this concept in mind, our strategy is to use transition metals and ligands that present an adequate number of binding sites to construct grid-type supramolecular compounds for the selective adsorption of dyes.

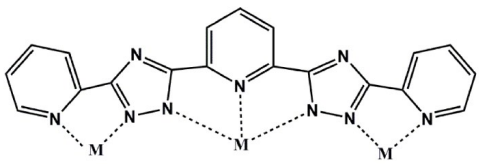

Figure.1 Schematic diagram and coordination mode of the ligand in complexes

In this work, we synthesize two grid-type architectures supported by the polynitrogen heterocyclic ligand 2,6-bis[5-(2-pyridinyl)-1H-triazol-3-yl]pyridine (H_2L; Figure 1)[15,18], which consists of three pyridyl rings linked by two triazolyl groups. The hydrothermal reaction of CuI with H_2L and $NH_3{\cdot}H_2O$ in methanol yielded an 11-membered mixed-valence copper cluster (complex **1**). While the reaction of $Cu(ClO_4)_2{\cdot}6H_2O$ with H_2L in methanol/water solution afforded a 15-membered mixed-valence copper cluster (complex **2**).

Experimental

Materials and Physical Measurements

All reagents and solvents were used as received from commercial supplies without further purification. Fourier

transform infrared (FTIR) spectra (KBr disk) were measured with a Vertex 70 FTIR on a spectrophotometer (4000–400cm^{-1}). Elemental analyses for C, H and N were obtained from a Perkin-Elmer 2400 elemental analyzer. Powder X-ray diffraction pattern (PXRD) was carried out on an EMPYREAN PANALYTICAL apparatus. UV-Vis absorption spectra were recorded at room temperature on a Hitachi U-3900 spectrophotometer.

Syntheses of complexes

$[Cu^{I}_4Cu^{II}_5(bptp)_6]\cdot(Cu^{I}I_2)_2(CH_3OH)_6(H_2O)_4$ (1)

A mixture of CuI (38.1 mg, 0.2 mmol), 2,6-H_2bptp (37.2 mg, 0.1 mmol), $NH_3\cdot H_2O$ (0.1 mmol), MeOH (12 mL) and a small amount of ascorbic acid were sealed in a 20 mL Teflon-lined reactor, which was heated at 140 ℃ for 120 h. Upon cooling to room temperature at a rate of 5 ℃h^{-1}, dark green crystals of 2 were obtained in 31.5% yield (7.69 mg) based on CuI Anal. Calcd (found) for $[Cu^{I}_4Cu^{II}_5(bptp)_6]\cdot 2(Cu^{II}_2)(CH_3OH)_6(H_2O)_4$ (M_w= 1831): C, 40.25 (39.35); H, 2.85 (2.70); N, 20.89 (20.65) %. IR data (KBr pellet, cm^{-1}): 3431 (s), 3027 (m), 2922 (m), 1603 (s), 1560 (m), 1489 (s), 1463 (m), 1410 (s), 1251 (w), 1137 (w), 1058 (w), 812 (m), 716 (s), 478 (w).

$[Cu^{I}_4Cu^{II}_{11}(bptp)_{10}(ClO_4)_2]\cdot(ClO_4)_4$ (2)

A mixture of $Cu(ClO_4)_2\cdot 6H_2O$ (74.09 mg, 0.2 mmol), 2,6-H_2bptp (37.2 mg, 0.1 mmol), MeOH (5 mL) and H_2O (5 mL) were sealed in a 20 mL Teflon-lined reactor, which was heated at 140 ℃ for 96 h. Upon cooling to room temperature at a rate of 5 ℃h^{-1}, dark green crystals of **1** were obtained in 24.1% yield (16.7 mg) based on $Cu(ClO_4)_2\cdot 6H_2O$. Anal. Calcd (found) for $[Cu^{I}_4Cu^{II}_{11}(bptp)_{10}(ClO_4)_2]\cdot(ClO_4)_4$ (M_w= 5202): C, 44.08 (44.85); H, 2.19 (1.92); N, 23.95 (22.98)%.

Results and discussion

Structure description of 1

Single crystal X-ray diffraction analysis reveals that complex **1** crystallizes in the monoclinic space group *C*2/*c* and consists of a nanonuclear copper cluster cation, a dinuclear copper cluster anion, six isolated methanol molecules and four water molecules. The nonanuclear copper cluster cation is stabilized by two groups of three roughly parallel heptadentate ligands arranged above and below the metal pseudo-planes (the two groups of ligands positioned in an almost perpendicular fashion), forming a [3×3] square grid as shown in Figure 1. In the [3×3] cation grid, there are three different types of coordination modes for copper ions: the central copper ion has octahedral coordination geometry; the four copper ions on the edge assume square-pyramidal coordination geometries and the four copper ions on the corner take tetrahedral manners. In the dinuclear copper cluster anion, two copper ions are surrounded by four I^- anions. The oxidation states of the copper ions were determined from the charge balance, coordination geometry and bond-valence sum (BVS) calculations[19, 20], which are listed in Table S3. Four copper ions on the corner in the [3×3] cation grid and two copper ions in the dinuclear cluster anion are Cu^{I}, the others are Cu^{II}. The sizes of the grid are presented in the schematic diagrams shown in Figure 2.

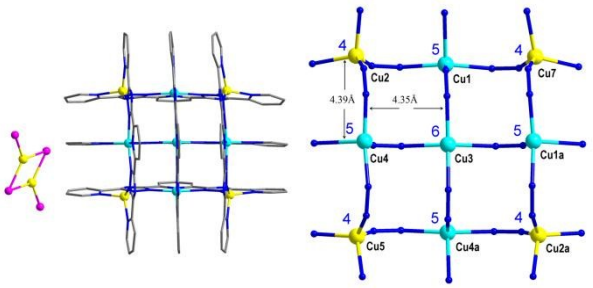

Figure.2 Crystal structure (left) and core structure (right) of **1**, solvent molecules and hydrogen atoms were omitted for clarity. Color code: C, gray; N, blue; I, pink; Cu^{II}, light blue; Cu^{I} yellow.

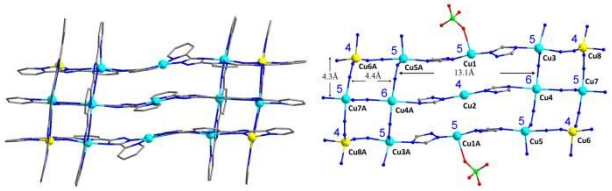

Figure.3 Crystal structure (left) and core structure (right) of **2**,hydrogen atoms were omitted for clarity. Color code: C, gray; N, blue; O, red; Cl, green; Cu^{II}, light blue; Cu^{I}, yellow.

Structure description of 2

Single crystal X-ray diffraction analysis reveals that complex **2** crystallizes in the triclinic space group *P*-1 and consists of a 15-membered copper cluster cation with four isolated perchlorate counterions. A structural representation for the cation is shown in Figure 2, the fifteen copper ions ligatured by ten L^{2-} ligands and two coordinated perchlorate are arranged in the [3×5] rectangular grid pattern. The ten ligands are arranged in two roughly parallel groups positioned in an almost perpendicular fashion above and below the metal pseudo-planes. In this [3×5] grid structure, there are five different types of coordination environments of the copper ions. The copper ion in the centre and the four copper ions in rectangular grid vertices are all four-coordinated with N_4 coordination environment; the former has a distorted square geometry while the latter adopt tetrahedral geometries. The eight copper ions on the edges of the grid present square-pyramidal coordination geometries, six with N_5 coordination environments while two with N_4O coordination environments. Two copper ions in central intersection of the grid exhibit distorted octahedral geometries with N_6 coordination environments. The oxidation states of the copper ions were determined from the charge balance, coordination geometry and bond-valence sum (BVS) calculations[19-20], which are listed in Table S5. The four copper ions in vertices of the rectangular grid are Cu^{I}, the others are Cu^{II}. The sizes of the grids are presented in the schematic diagrams shown in Figure 3.

Dye adsorption experiments

As the grid-type architectures described above, we probed the ability of these two complexes to remove different pollutant dyes from water. Four dyes (Figure S1, methylene blue (MB), methyl orange (MO), rhodamine B (RB) and congo red (CR)) with different sizes and charges which perhaps would be absorbed were chosen as models. Therefore, dye adsorption experiments with **1** and **2** have been carried out. Typically, 10 mg of adsorbent complexes were immersed in 50 mL of aqueous dye solutions containing a 2×10^{-5}mol L^{-1} of dyes in the dark at room temperature; the adsorption system was maintained under controlled stirring. During given time, the abilities of complexes to absorb dyes from aqueous solution were determined through UV-Vis absorption spectroscopy.

According to UV-Vis absorption spectroscopy, **1** showed no dye adsorption under the described conditions regardless of the dye used, which is in accordance with the small grid size of ~4.3 Å estimated from crystal structure analysis. As shown in Figure 4, spectroscopic study of **2** indicated that MO was almost completely absorbed by the absent within a certain period of time. It is worth noting that no or very small amount of RB, MB or CR were absorbed during the assay, which indicated that **2** can efficiently and selectively adsorb dyes and achieve the purpose of separation of dyes.

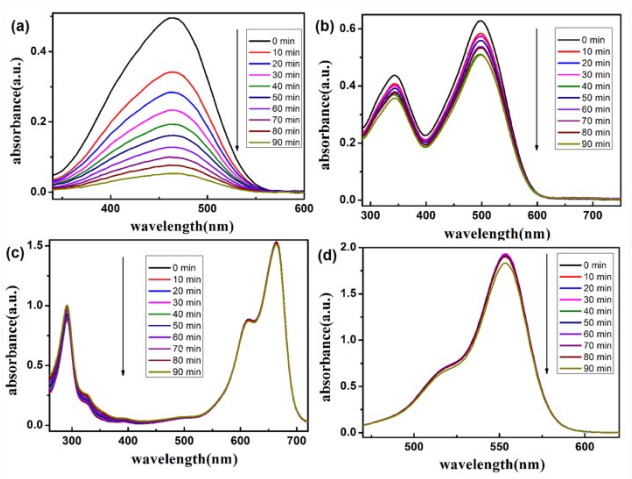

Figure.4 UV-Vis spectra of aqueous solutions of dyes with **2**: (a) MO, (b) CR, (c) MB and (d) RB.

To evaluate the adsorption activity of complex **2**, the UV-Vis absorption spectrum of MO solution in the presence of **2** was conducted. The amount of MO adsorbed by the complex was calculated based on a mass balance equation[21] as given by: $q_e=(c_0-c_{eq})\times V/w$, where q_e is the equilibrium adsorption capacity per gram dry weight [mmol g^{-1}] of the adsorbent ; c_0 and c_{eq} are the initial and final or equilibrium concentrations [mmol L^{-3}] of MO in the solution; V is the volume [L^{-3}] of the solution; and w is the dry weight [g] of the complex. The adsorption capacity of the absorbent **2** is 0.09 mmol g^{-1} (29.5 mg g^{-1}). As shown in Figure 4, it is found that the adsorption rate of 2×10^{-5}mol L^{-1} MO (50 mL) solution reached to 90% in 90 min. In order to further confirm the effect of the absorbent concentration in this absorb system, we changed the concentration of the complex **2** in the control experiment. It is indicated that the uptake capacity of MO increased with the increase of the complex concentration (Figure 5). Noticeably, the grids with appropriate sizes containing in compound **2** were extremely selective in the adsorption of the methyl orange (MO). Although the adsorption capacity of this grid-type architecture is lower than that of other adsorbents, especially compared with MOFs[11], the exploration about the adsorption ability of this grid-type supramolecular is of great significance for it develops a new kind of adsorption materials and provides a special direction for the application of this structure.

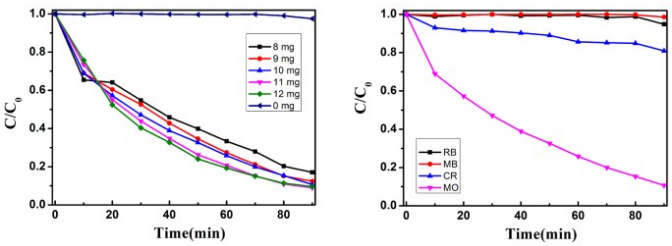

Figure.5 Concentration changes of MO with time in the presence of different concentration of **2**(Left); Concentration changes of MB, RB, MO, and CR with time in the presence of **2**(Right).

In addition, the mechanism for the selective adsorption can be explained from two aspects. Firstly, the grids in complex **2** are positively charged while MO molecules (Figure S2) are negatively charged. Thus there exists strong electrostatic interaction between them. Naturally, MO as an anionic dye can enter into the pores of **2**, while MB and RB as a cationic anionic dye cannot. Secondly, the size of MO molecules is much smaller than that of the other anionic dye CR (Figure S2) and is just in accordance with the small grid size of ~4.3 Å of complex **2**. Therefore the strong electrostatic interaction and topological matching form the host–guest interaction between MO and complex **2**. Then the MO molecules could perfectly access into the grids of complex **2**, and grid-type architectures of complex **2** could selectively and efficiently adsorb MO.[10-11]

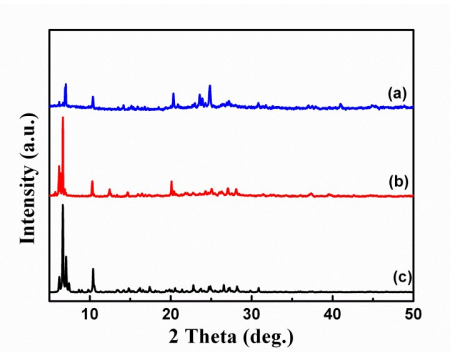

Figure.6 PXRD patterns of: experimental data for **2** (a), experimental data for **2** after adsorption experiment (b) and simulated data for **2** (c).

The adsorption of MO was also assessed by IR but that the corresponding results were not very convincing (Figure S3).

While, the XRD pattern of the complex **2** regenerated from adsorption experiment was almost similar to that of as-synthesized sample and simulated one of complex **2** (Figure 6). The slight difference may be derived from the impurity of sample and crystal lattice distortion during the adsorption process. These results can reveal that the grid architecture remained almost intact in aqueous solution of the organic dyes.

Conclusions

In conclusion, two novel grid-type architectures composed of mixed valence copper ions were prepared from the hydrothermal reaction of a polynitrogen heterocyclic ligand with Cu^{I} or $Cu(ClO_4)_2{\cdot}6H_2O$, respectively. The 11-numbered copper complex **1** possesses [3×3] grid structure with six Cu^{I} and five Cu^{II}, while the 15-numbered copper complex **2** has [3×5] grid structure with four Cu^{I} and eleven Cu^{II}. The UV-Vis adsorption spectroscopy showed that the complex **2** would efficiently and selectively adsorb MO molecules. We believe that the selective adsorption of grid superstructure is helpful for the design and application of this material, such as in the controlled separation and delivery.

Acknowledgements

We would like to kindly acknowledge the NSFC (21361016) and Inner Mongolia Foundation for Natural Science (2013ZD09) for financial support.

Notes and references

[a] College of Chemistry and Chemical Engineering Inner Mongolia University Hohhot,010021, P. R. China. E-mail: cezlliu@imu.edu.cn; Fax: +86-471-4992147; Tel: +18686029088.

[b] Inner Mongolia Key Lab of Fine Organic Synthesis, Inner Mongolia University, Hohhot, P. R. China

† X-ray crystallographic data for the structures of complex1, 2 have been deposited with the Cambridge Crystallographic Data Centre (CCDC No. 1032585 for complex 1, CCDC No. 1032586 for complex 2).

Electronic Supplementary Information (ESI) available: BVS values, selected bond distances and bond angles. For ESI and crystallographic data in CIF or other electronic format see DOI: 10.1039/b000000x/

1. O. S. Ayanda, O. S. Fatoki, F. A. Adekola and B. J. Ximba, *J Chem Technol Biotechnol*, 2013, 88, 2201-2208.
2. H. Chen, A. Zhong, J. Wu, J. Zhao and H. Yan, *Ind Eng Chem Res*, 2012, 51, 14026-14036.
3. L. Zhou, C. Gao and W. Xu, *Acs Appl Mater Interfaces*, 2010, 2, 1483-1491.
4. C. K. Lee, S. S. Liu, L. C. Juang, C. C. Wang, K. S. Lin and M. D. Lyu, *J Hazard Mater*, 2007, 147, 997-1005.
5. A. G. Espantaleón, J. A. Nieto, M. Fernández and A. Marsal, *Appl Clay Sci*, 2003, 24, 105-110.
6. Y. Yu, Y.-Y. Zhuang, Z.-H. Wang and M.-Q. Qiu, *Ind Eng Chem Res*, 2003, 42, 6898-6903.
7. Y. Al-Degs, M. A. M. Khraisheh, S. J. Allen and M. N. Ahmad, *Water Res*, 2000, 34, 927-935.
8. E. F. Molina, R. L. T. Parreira, E. H. De Faria, H. W. P. de Carvalho, G. F. Caramori, D. F. Coimbra, E. J. Nassar and K. J. Ciuffi, *Langmuir*, 2014, 30, 3857-3868.
9. F. Rodríguez-Llansola, B. Escuder, J. F. Miravet, D. Hermida-Merino, I. W. Hamley, C. J. Cardin and W. Hayes, *Chem Commun*, 2010, 46, 7960.
10. H.-N. Wang, F.-H. Liu, X.-L. Wang, K.-Z. Shao and Z.-M. Su, *J Mater Chem A*, 2013, 1, 13060-13063.
11. Z. Hasan and S. H. Jhung, *J Hazard Mater*, 2014, 283C, 329-339.
12. M. Ruben, J. Rojo, F. J. Romero-Salguero, L. H. Uppadine and J. M. Lehn, *Angewandte Chemie*, 2004, 43, 3644-3662.
13. L. K. Thompson, O. Waldmann and Z. Xu, *Coordin Chem Rev*, 2005, 249, 2677-2690.
14. T. Shiga, T. Matsumoto, M. Noguchi, T. Onuki, N. Hoshino, G. N. Newton, M. Nakano and H. Oshio, *Chem Asian J*, 2009, 4, 1660-1663.
15. X. Bao, W. Liu, L. L. Mao, S. D. Jiang, J. L. Liu, Y. C. Chen and M. L. Tong, *Inorg Chem*, 2013, 52, 6233-6235.
16. H. Sato, L. Miya, K. Mitsumoto, T. Matsumoto, T. Shiga, G. N. Newton and H. Oshio, *Inorg Chem*, 2013, 52, 9714-9716.
17. A. R. Stefankiewicz, G. Rogez, J. Harrowfield, M. Drillon and J.-M. Lehn, *Dalton Trans*, 2009, DOI: 10.1039/b902262g, 5787.
18. X. Bao, W. Liu, J.-L. Liu, S. Gómez-Coca, E. Ruiz, and M.-L. Tong, *Inorg Chem*, 2013, 52, 1099-1107.
19. I. D. Brown and D. Altermatt, *Acta Cryst B*, 1985, 41, 244-247.
20. W. Liu and H. H. Thorp, *Inorg Chem*, 1993, 32, 4102-4105.
21. F. Pu, X. Liu, B. Xu, J. Ren and X. Qu, *Chem Eur J*, 2012, 18, 4322-4328.

